From SED to line suppression:

Probing the physics of the X-ray-weak WLQ SDSS J101353.45+492758.1

Laetitia Gibaud

WYDZIAŁ FIZYKI
UNIWERSYTET W BIAŁYMSTOKU

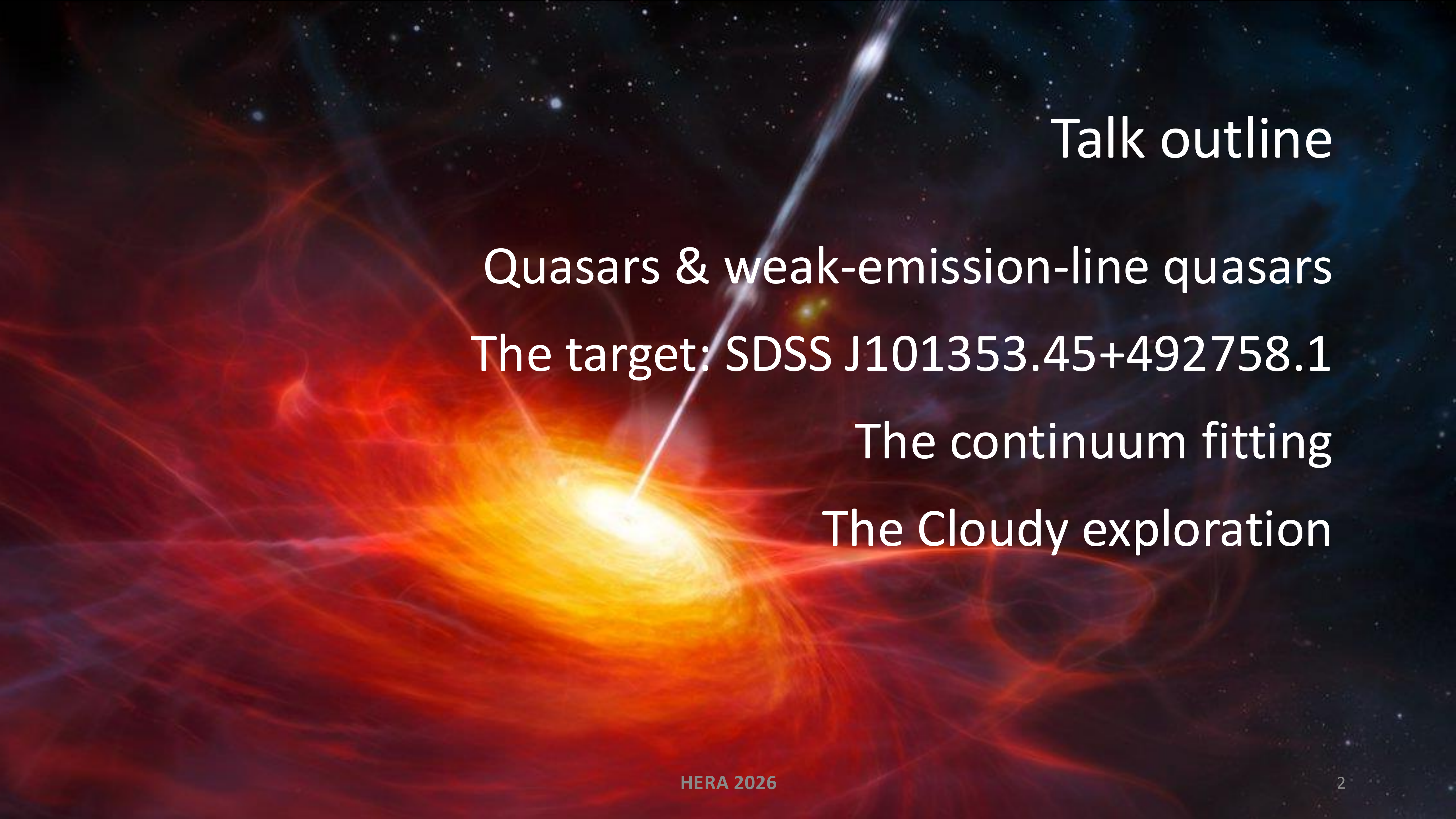

Talk outline

Quasars & weak-emission-line quasars

The target: SDSS J101353.45+492758.1

The continuum fitting

The Cloudy exploration

Quasars & weak-emission-line quasars

Quasars with unusually weak emission lines
=> Challenge standard BLR/accretion paradigms

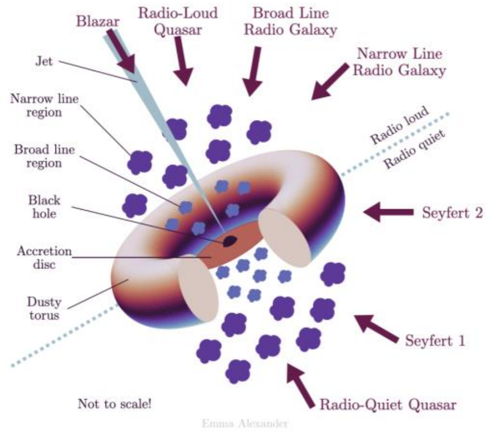

Adapted from Urry & Padovani 1995

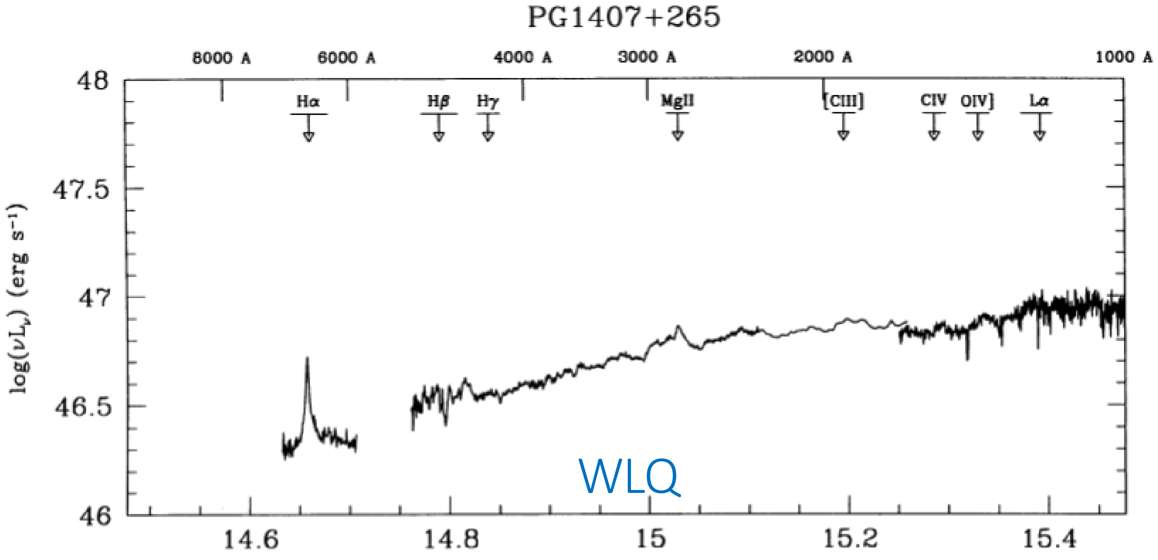

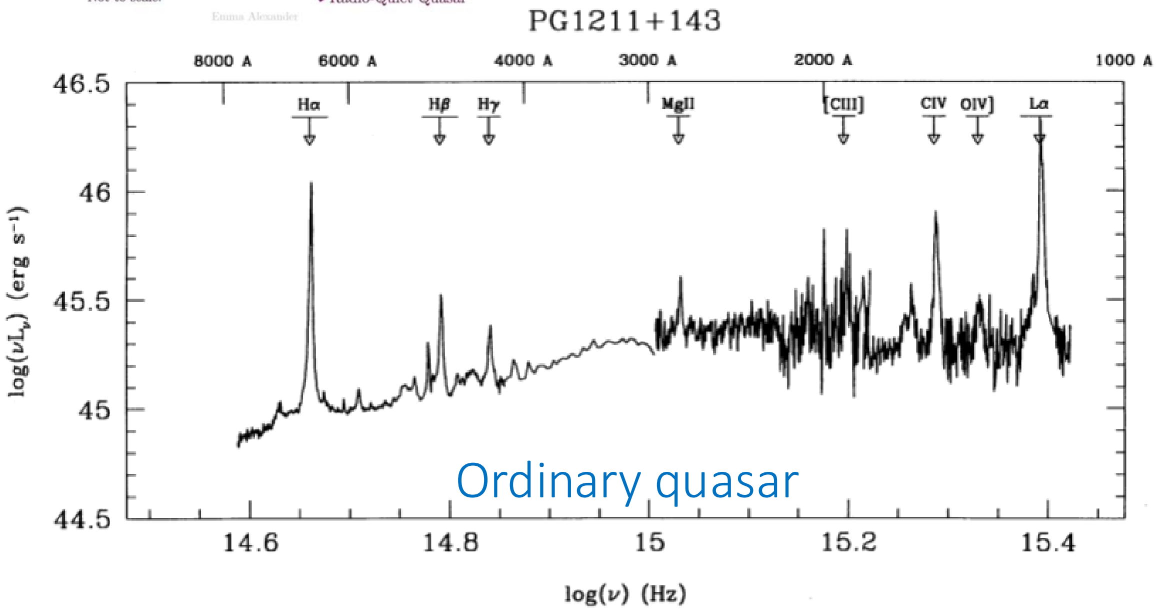

McDowell et al. 1995

Why should we care about WLQs?

EW distribution of high and low ionization lines from Cheng et al. 2025

C IV λ1549 EW(Å)

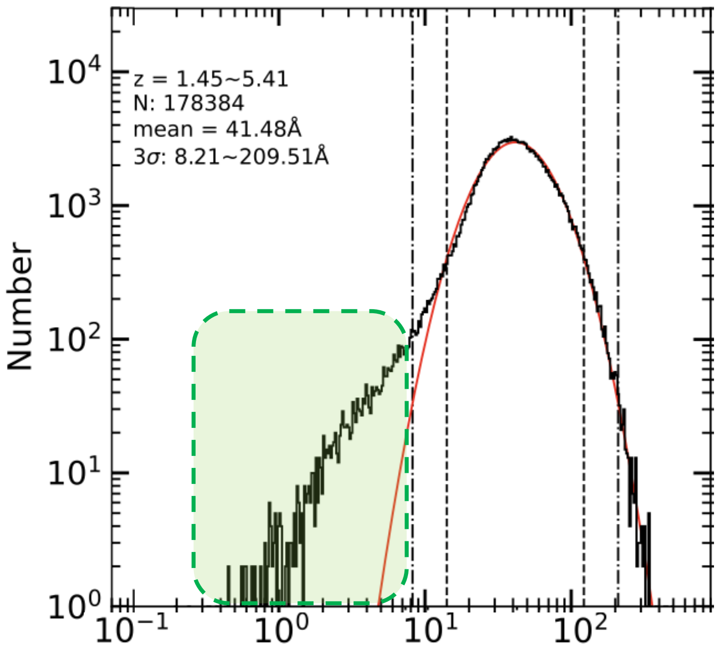

C III] λ1909 EW(Å)

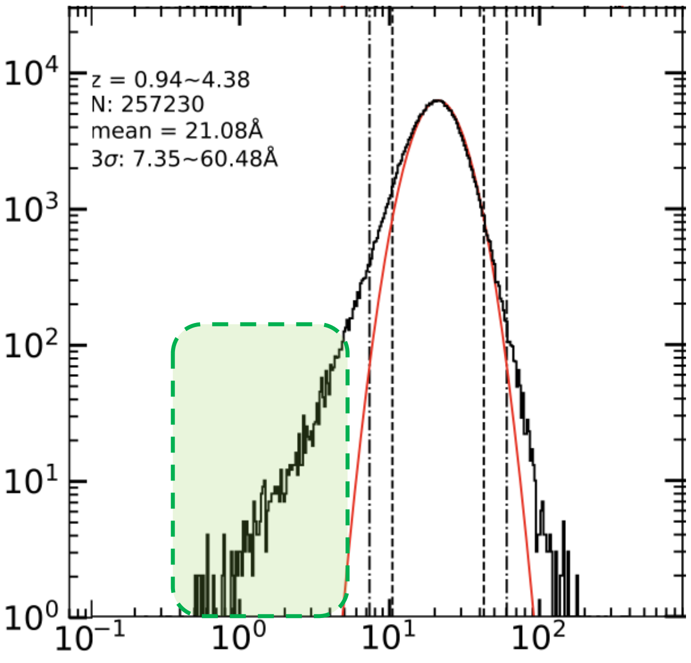

Mg II λ2798 EW(Å)

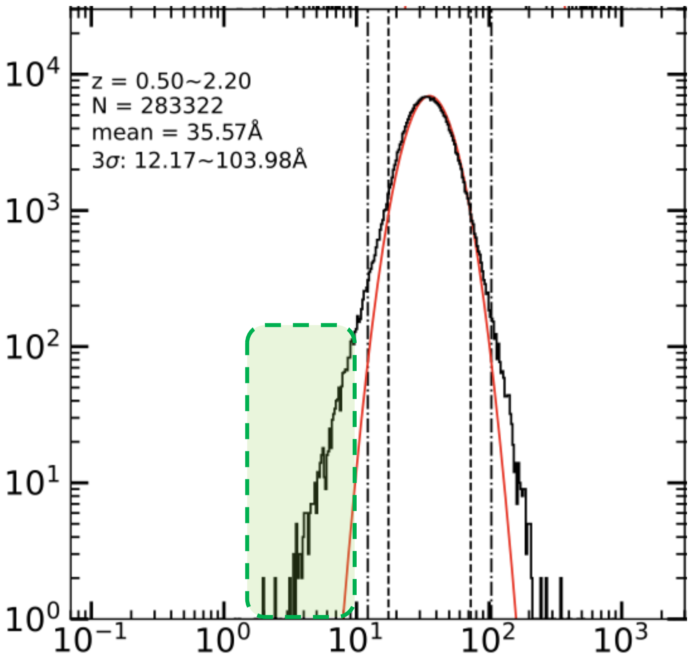

A few possible explanations

Anemic or underdeveloped BLR and/or evolutionary effects

Super-Eddington accretion

Shielding gas

The target: SDSS J101353.45+492758.1

z = 1.64 ; D = 4691.20 Mpc

L = 1.06 x 10^{46} erg/s

$L_{X(0.5\text{-}10\ keV)}$ = 2.25 x 10^{41} erg/s (Young et al. 2009)

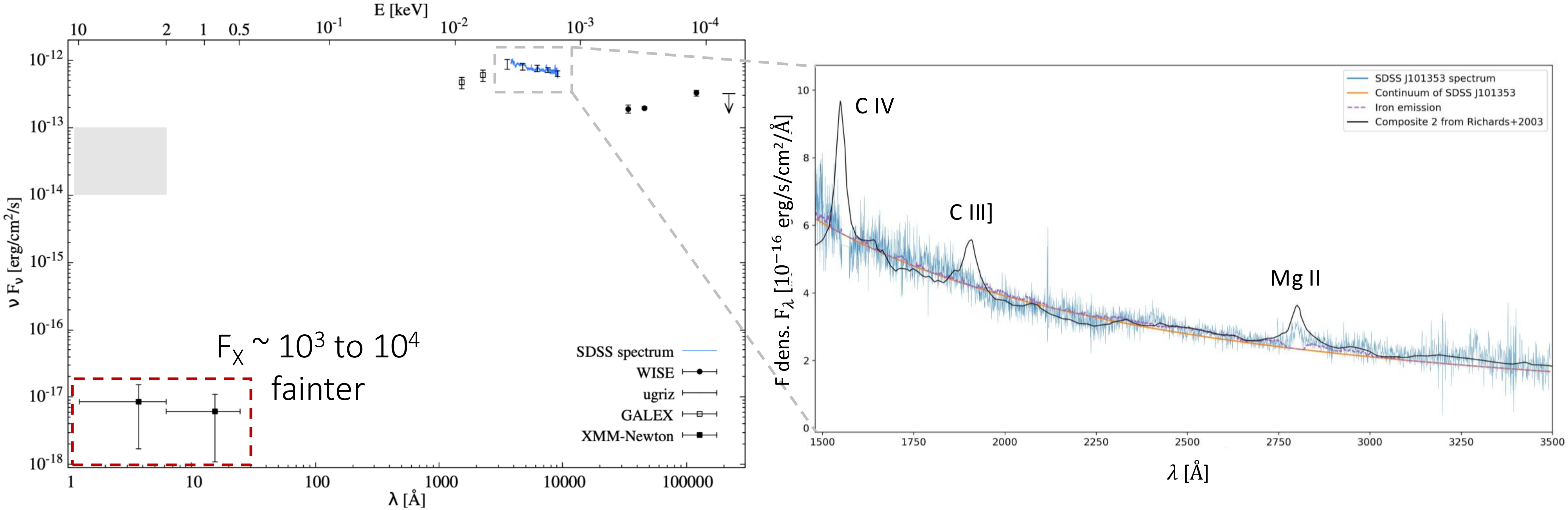

Mg II emission line

Key ideas:

- Extraction of emission line information
- BH's parameters determination as baseline for fitting process

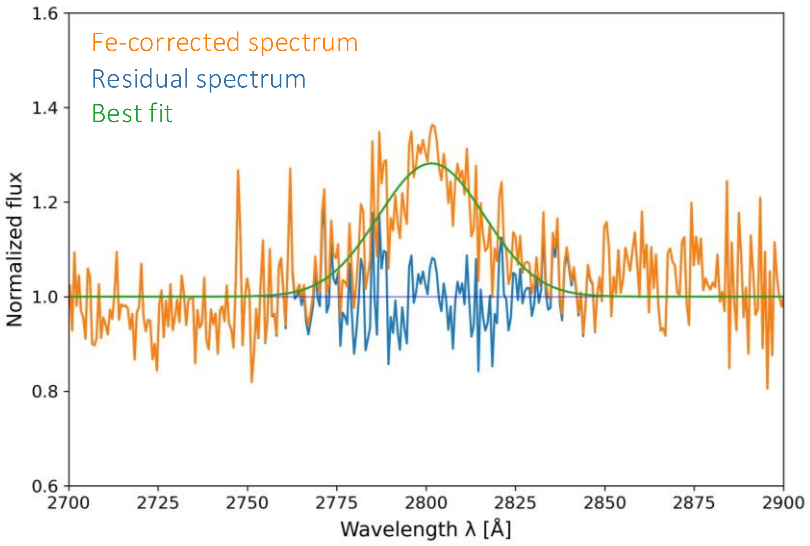

Rest-frame Mg II properties of SDSS J101353 (Gibaud et al. 2026)

λ (Å)	FWHM (km s^{-1})	REW (Å)
2801.63 ± 0.90	3875.13 ± 250.99	10.89 ± 0.57

$$M_{SMBH} = 10^{6.86} \left[\frac{\mathrm{FWHM(Mg\ II)}}{1000\ \mathrm{km/s}}\right]^2 \left[\frac{\lambda L_\lambda(3000\ \text{Å})}{10^{44}\ \mathrm{erg/s}}\right]^{0.5}$$

(Vestergaard & Osmer 2009)

$$\dot{m} = \frac{L_{bol}}{L_{Edd}} \quad \text{with} \quad L_{Edd} = 1.25 \times 10^{38}\ \mathrm{erg\ s^{-1}} (M/M_\odot)$$

RESULTS:

- $M_{SMBH} = (4.95 \pm 0.64) \times 10^8\ M_\odot$
- $\dot{m} = 0.17$

Estimations susceptible to bias!
Marculewicz & Nikolajuk (2020)

The continuum fitting

Models to explore the geometry

Model 1

A simple geometry:

- relativistic thin disk (**kerrbb**, Li et al. 2005)
- power law
- starlight component (Polletta et al. 2007)
- torus component

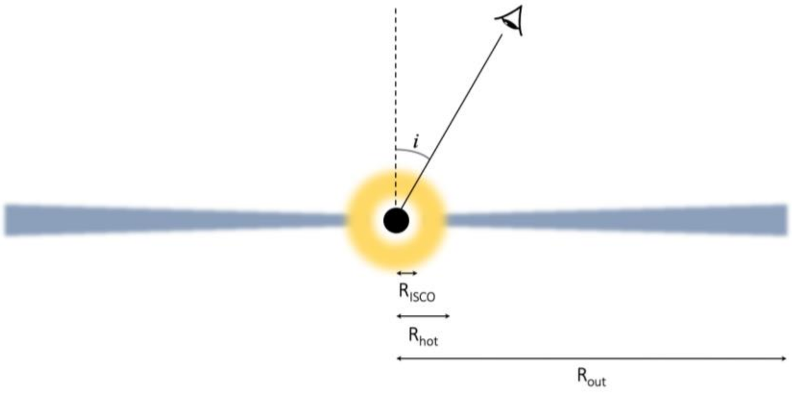

Model 2

A more complex geometry:

- accretion disk + warm Comptonization region (**relagn**, Hagen & Done 2023)
- starlight component (Polletta et al. 2007)
- torus component

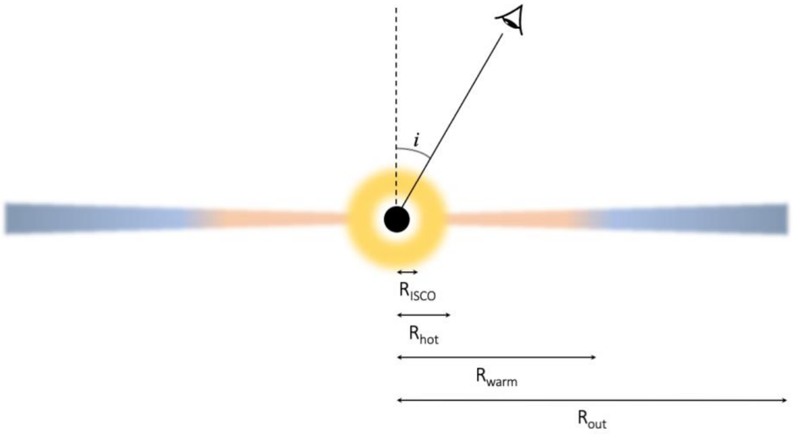

Broadband SED fit assuming a simple geometry: model 1

Hot corona (hot plasma
T~10^9 K)
-> **PL**

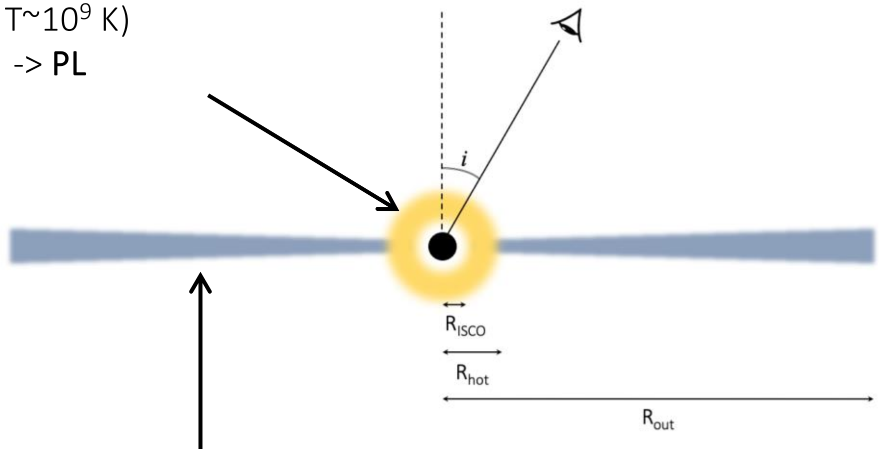

AD -> relativistic thin disk
model **kerrbb**

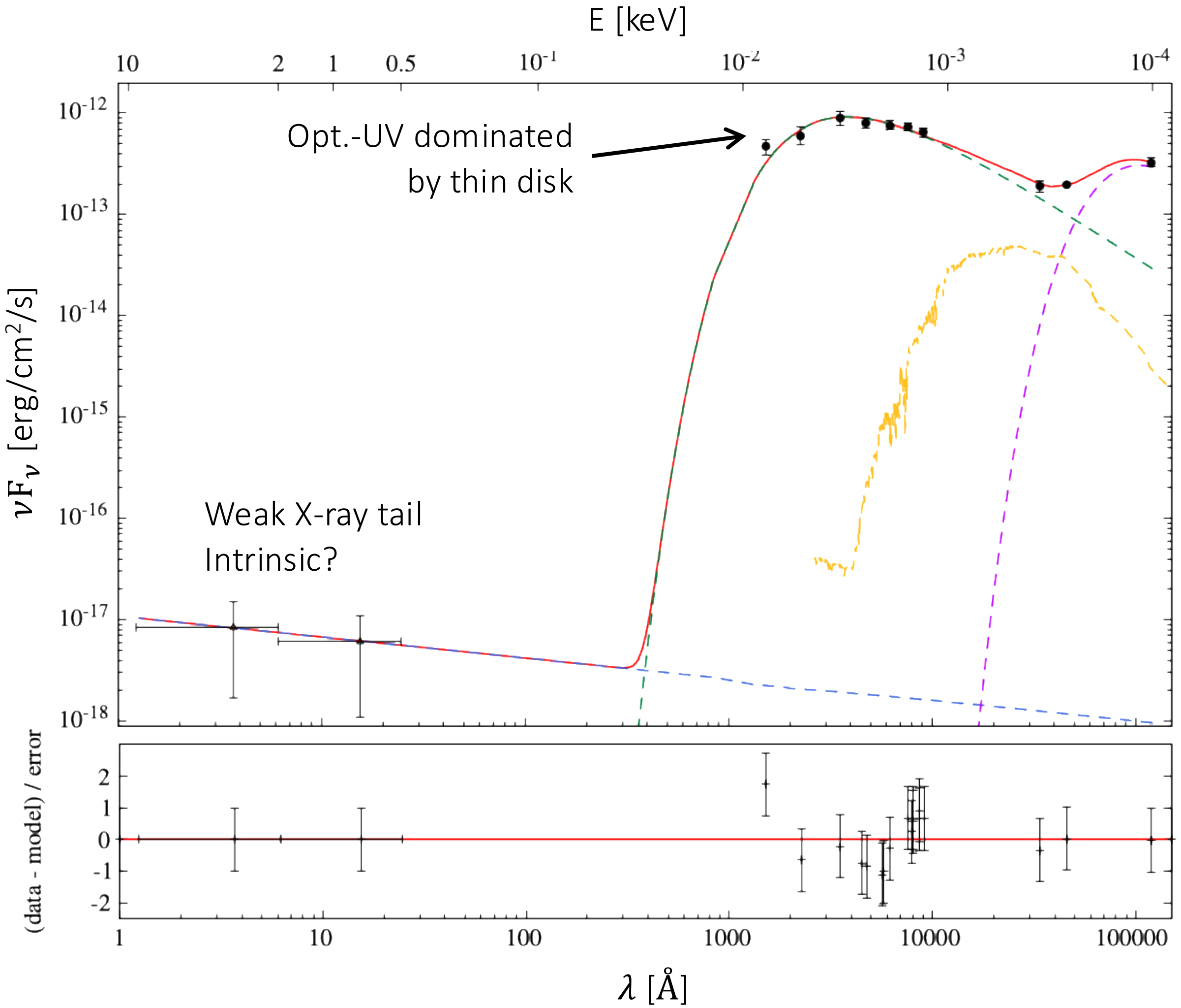

AD + compact weak hot corona

Broadband SED fit assuming a complex geometry: model 2

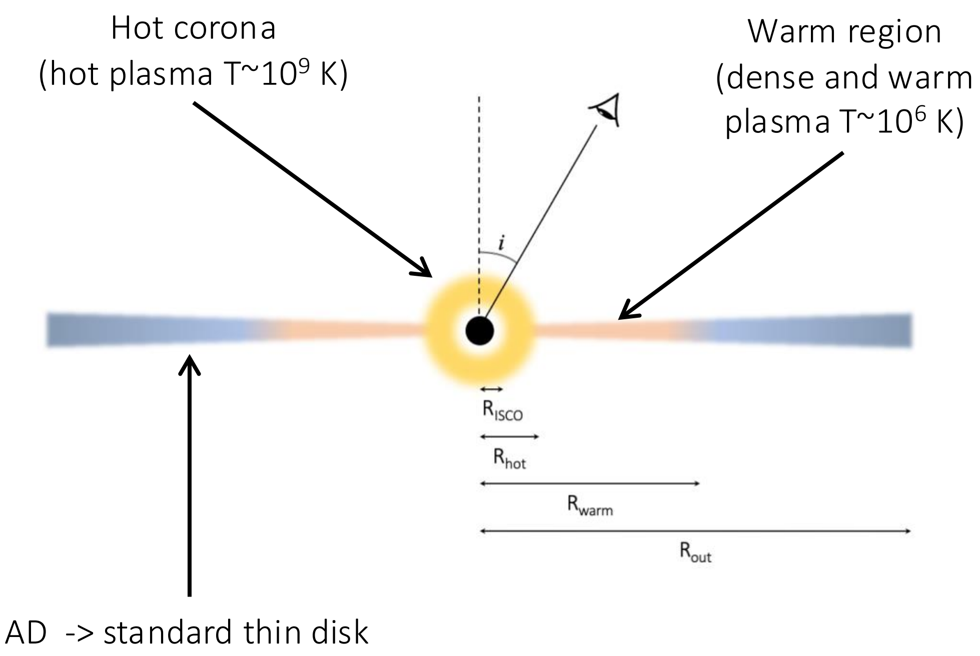

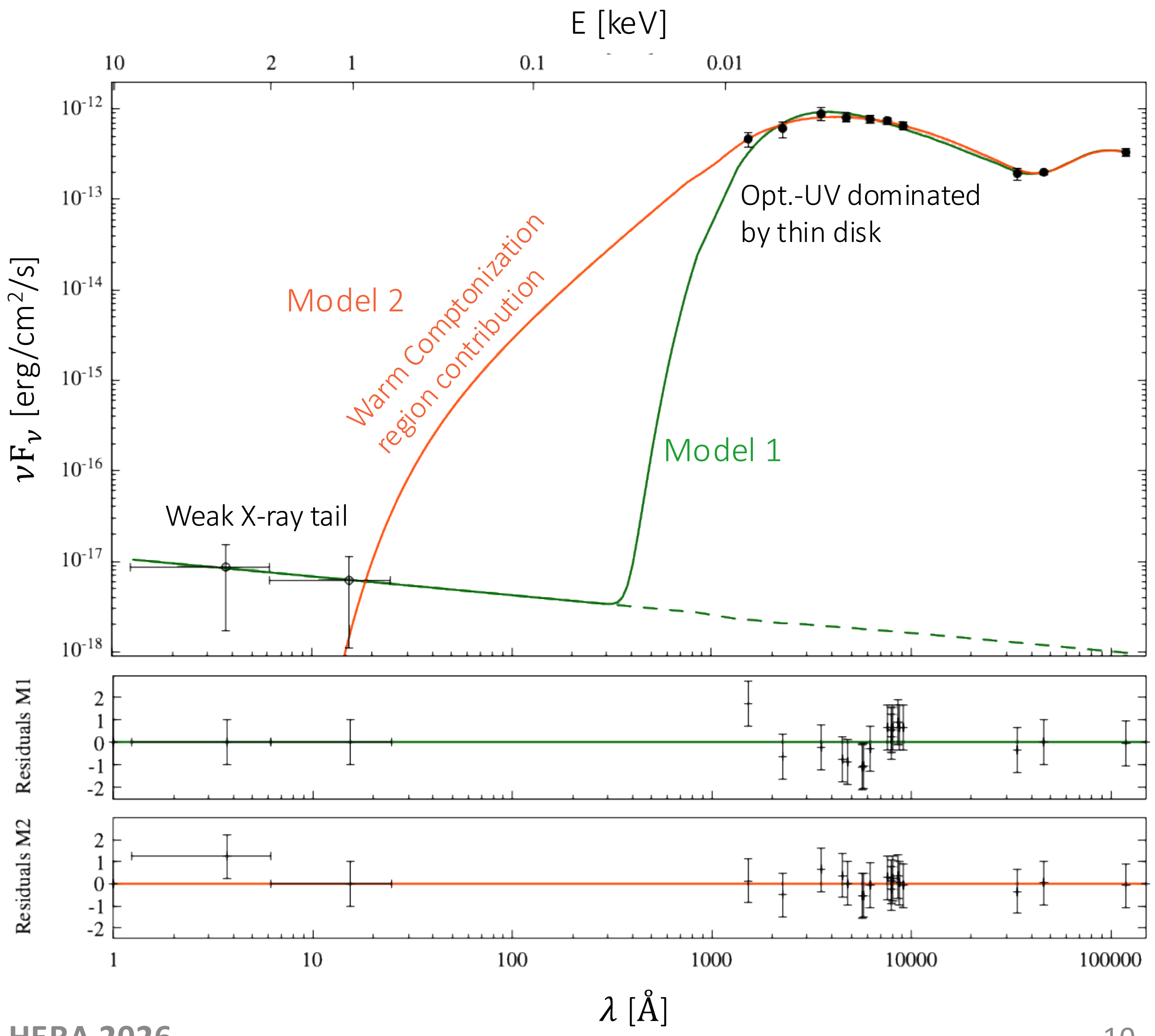

Broadband SED fit assuming a complex geometry: model 2

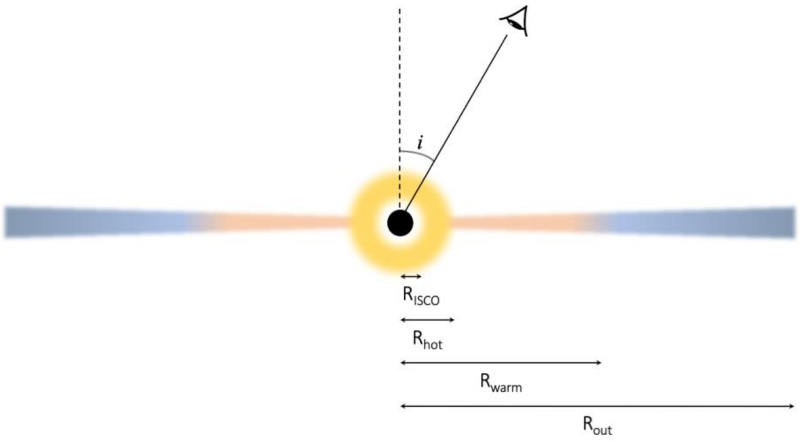

Warm region parameters:

- $kT_{e,warm} \approx 0.19^{+0.06}_{-0.09}$ keV
- $\Gamma_{warm} \approx 3.83^{+0.47}_{-0.19}$
- $R_{warm} \approx 34^{+10}_{-7}$ Rg

Consistent with an optically thick warm corona

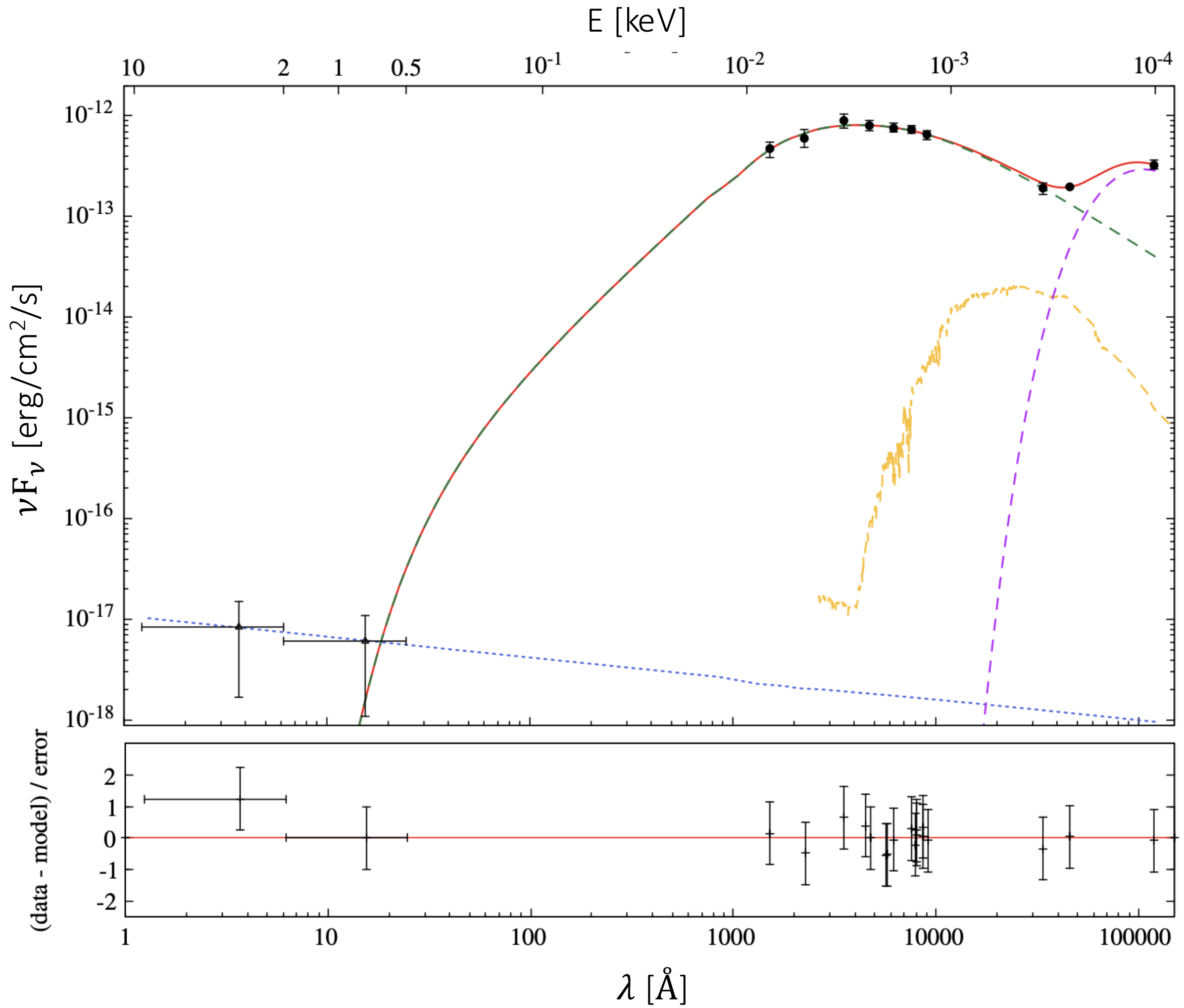

Fitting results

Gibaud et al. 2026

Model	M_{BH} (10^9 $M_\odot$)	$\dot{m}^a$	$\Gamma_{hot}{}^b$	$\Gamma_{warm}{}^c$	Starlight (10^{-17})	$kT_{e,torus}$ (K)	χ^2/d.o.f.
Model 1	$2.05^{+0.37}_{-0.30}$	$0.087^{+0.005}_{-0.006}$	1.8 ± 0.8	–	5.18 ± 3.93	934.16 ± 98.64	10.31/13
Model 2	$1.90^{+0.28}_{-0.26}$	$0.155^{+0.027}_{-0.025}$	1.8 fixed	$3.83^{+0.47}_{-0.19}$	1.83 ± 0.87	913.27 ± 30.18	3.69/12

Notes. Model 1a: **kerrbb** + power law. Model 1b: accretion disk + compact weak hot corona using **relagn**. Model 2: warm region contribution to Model 1b using **relagn**. [a]Accretion rate $\dot{m} = \dot{M}/\dot{M}_{Edd}$. [b]Photon-index in the 1–10 keV energy range. [c]Photon-index in the 0.1–1 keV energy range.

Massive BH
Moderate accretion rate

Hot corona

Warm corona

Typical hot thermal dust emission in WLQs ranges from 870 K to 1240 K according to Diamond-Stanic et al. (2009).

Proposed interpretations

Ultrasoft state in XRBs:

- High Edd. accretion rate (~ 0.5)
- Thermal disk fraction -> 80-90% of the tot. flux
- Weak hot corona => weak X-rays
- Radio quenched

Spectral state in SDSS J101353:

- **does not require** high-Eddington accretion
- has an intrinsically weak hot corona => may represent an AGN analogue of the **ultrasoft state** observed in XRBs, but with a smaller accretion rate

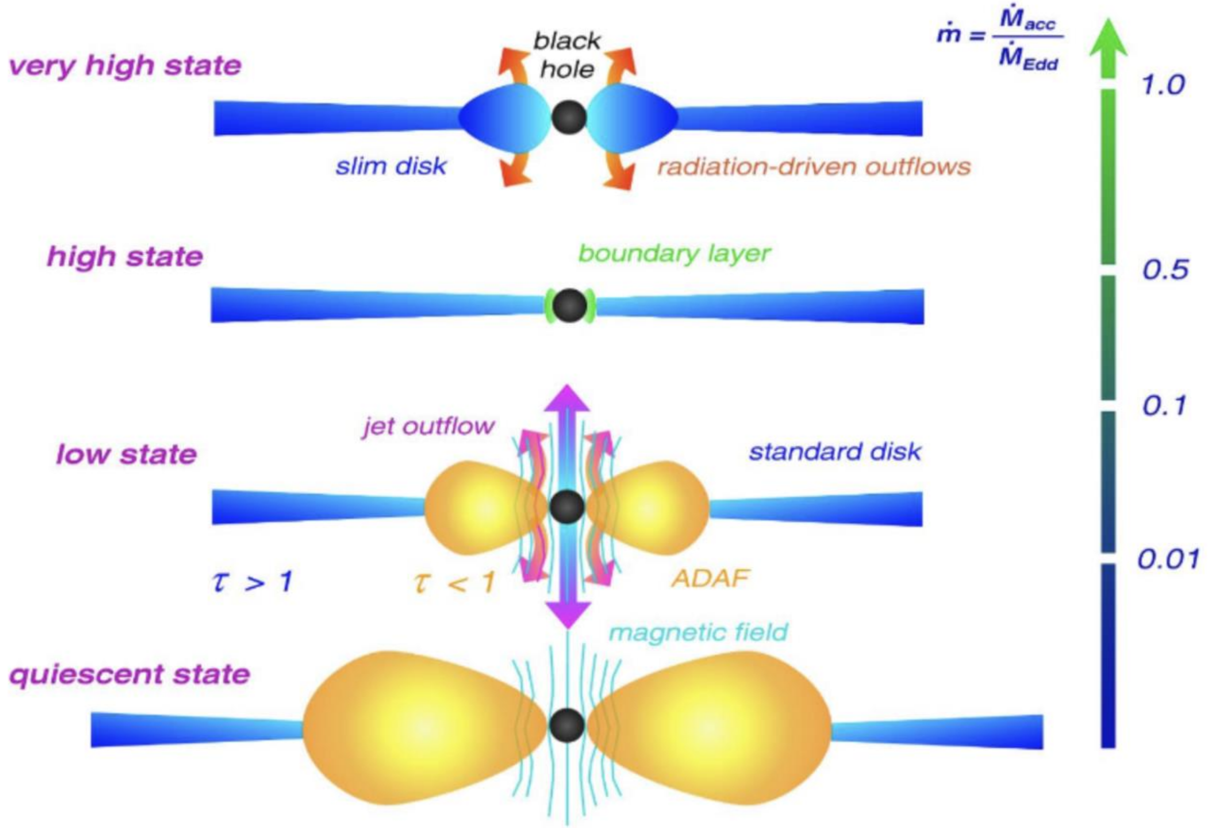

Credit: Muller 2004

The Cloudy exploration

Photoionization simulations performed with Cloudy code (e.g., Chatzikos et al. 2023)

Methodology used for this case:

- Input SEDs from models 1 & 2
- Run grid of simulations assuming a **single BLR cloud**, over:
  - Column densities N_H, from 10^{22} to 10^{24} cm^{-2}
  - H densities n_H, from 10^9 to 10^{12} cm^{-3}
  - Distances R from the central engine, from 10^{14} to 10^{21} cm

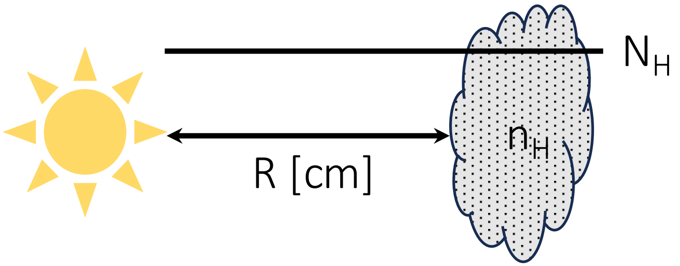

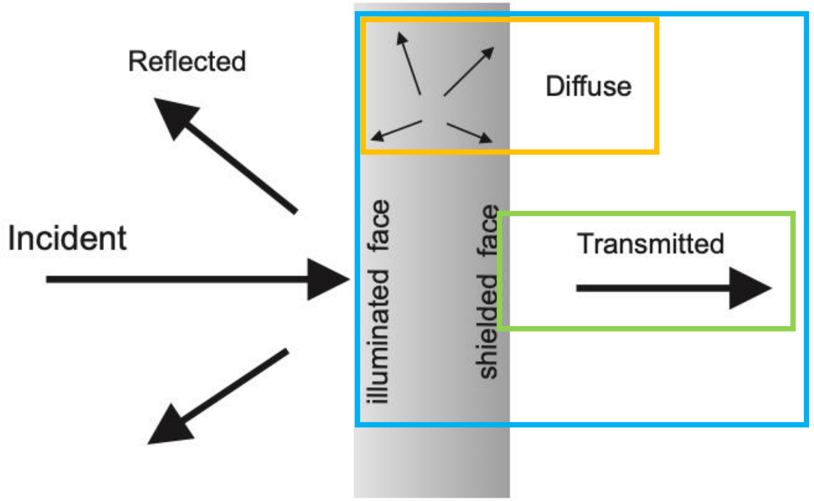

Source: Hazy documentation

Luminosity ratios for **model 1**

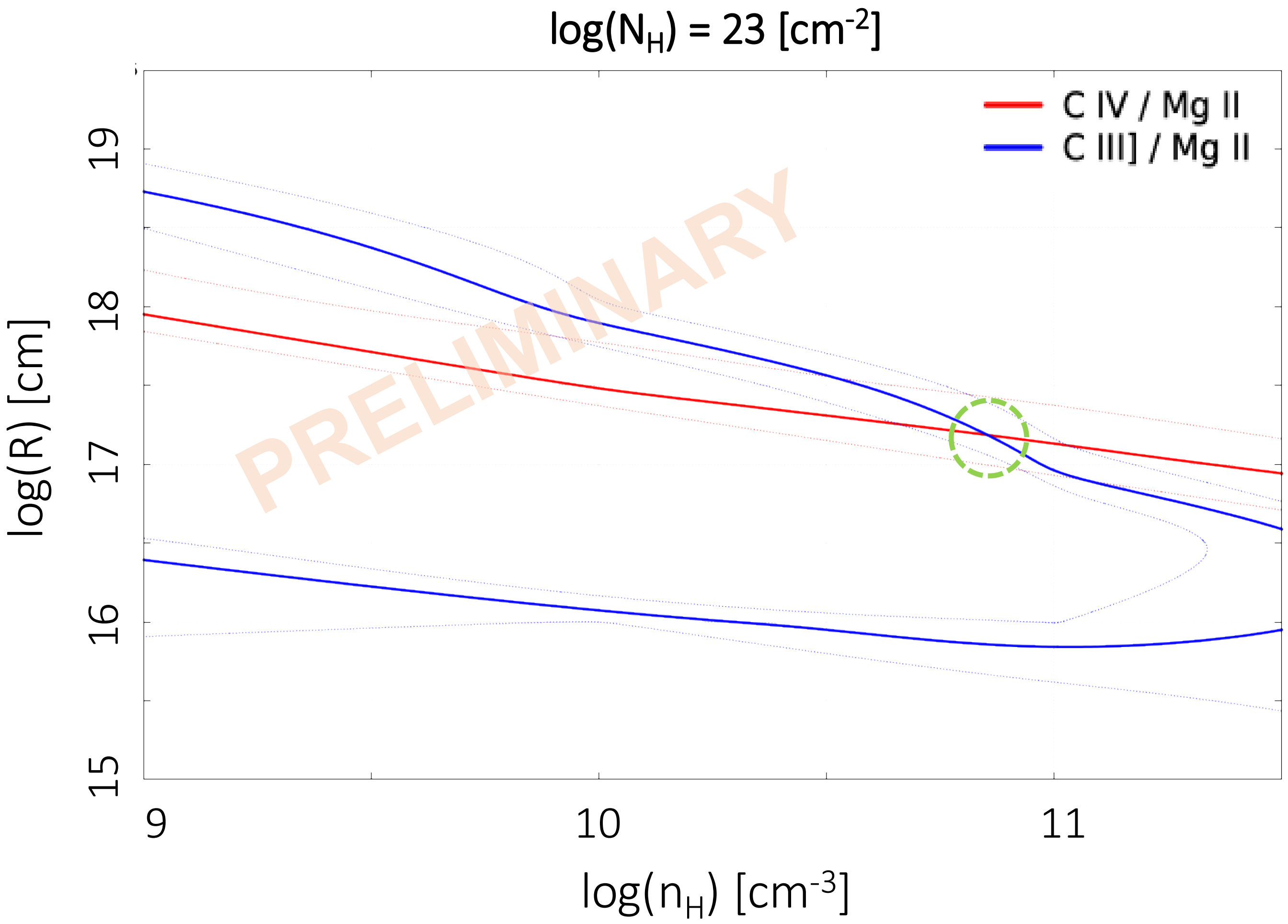

The 2 luminosity ratios agree with a narrow parameter range:

- log(n_H) ≈ **10.9** [cm^{-3}]
- log(R) ≈ **17.2** [cm]

Luminosity ratios for **model 2**

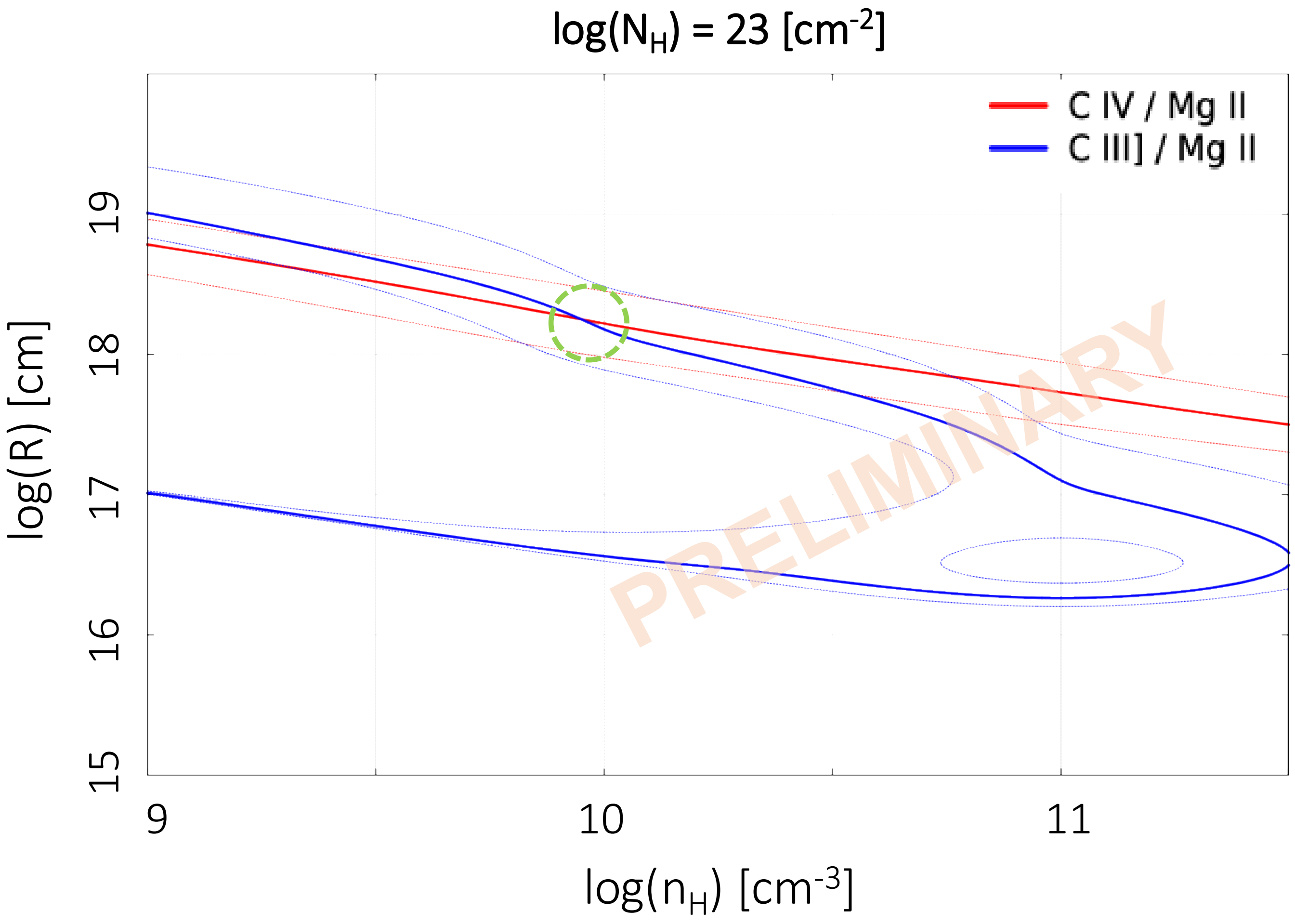

The 2 luminosity ratios agree with a narrow parameter range:

- log(n_H) ≈ **10.0** [cm^{-3}]
- log(R) ≈ **18.2** [cm]

EW of MgII emission line for **model 1**

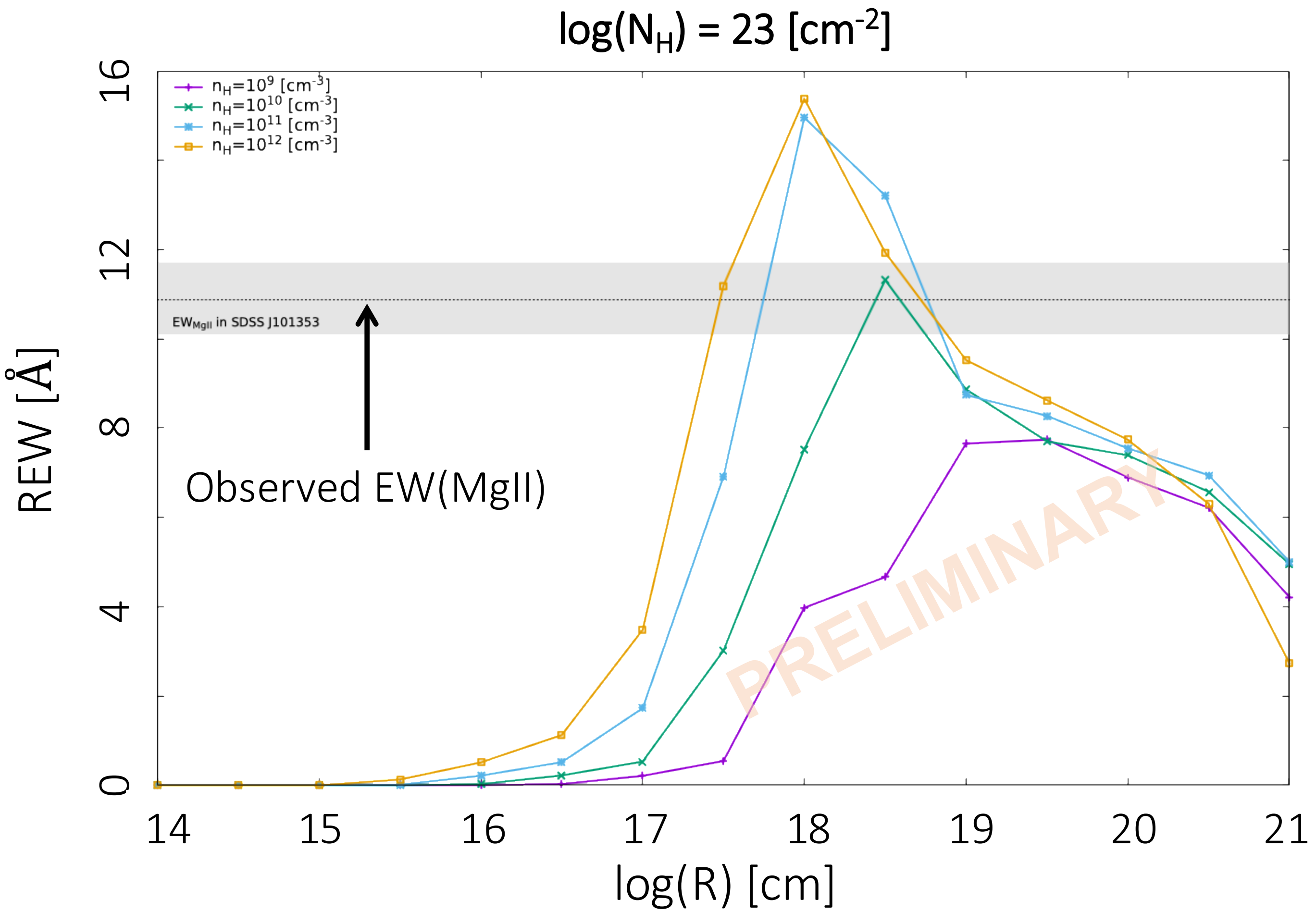

$n_H=10^9$ [cm^{-3}]
$n_H=10^{10}$ [cm^{-3}]
$n_H=10^{11}$ [cm^{-3}]
$n_H=10^{12}$ [cm^{-3}]

→ CF=7%

EW of MgII emission line for **model 2**

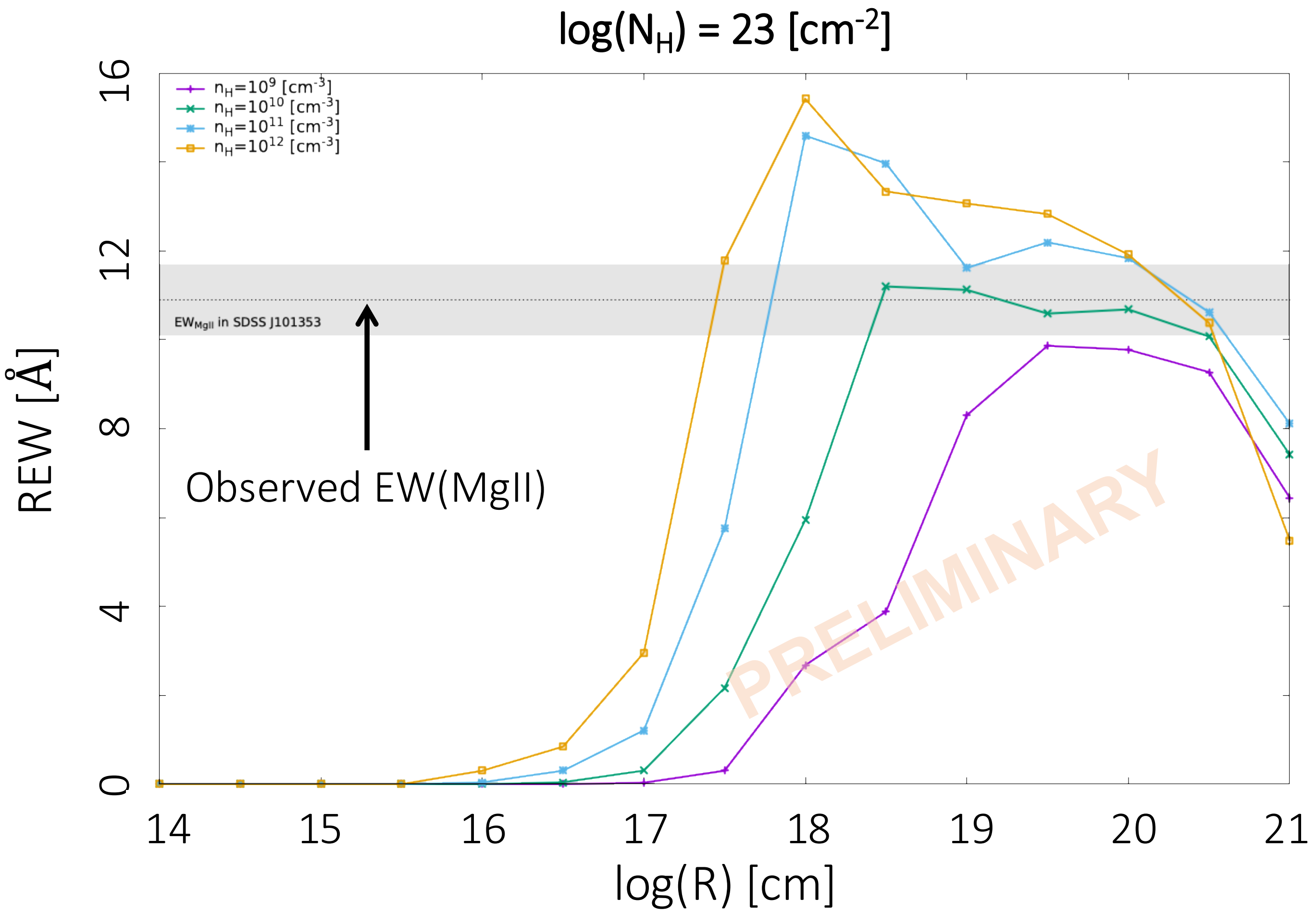

$n_H = 10^9$ [cm^{-3}]
$n_H = 10^{10}$ [cm^{-3}] → CF=5%
$n_H = 10^{11}$ [cm^{-3}]
$n_H = 10^{12}$ [cm^{-3}]

Conclusions

- The ultrasoft-state interpretation provides a physically plausible explanation that naturally accounts for the observed SED of SDSS J101353
- **Inefficient** and/or **compact** hot corona
- Evidence of a warm corona till 34 Rg (model 2)
- SDSS J101353 **does not accrete at high-Eddington rate (only at** $\dot{m} \approx 0.1$**)**

From photoionization simulations:

- The BLR is located around 10^{17} to 10^{18} cm from the central engine
- Small covering factors are required to reproduce the observed EWs in WLQs

THANK YOU!

The obscuration scenario

An alternative explanation for the X-ray weakness in SDSS J101353 is that the observed hard X-ray spectrum does not represent the intrinsic coronal emission, but rather its reflection from obscuring material along the line of sight.

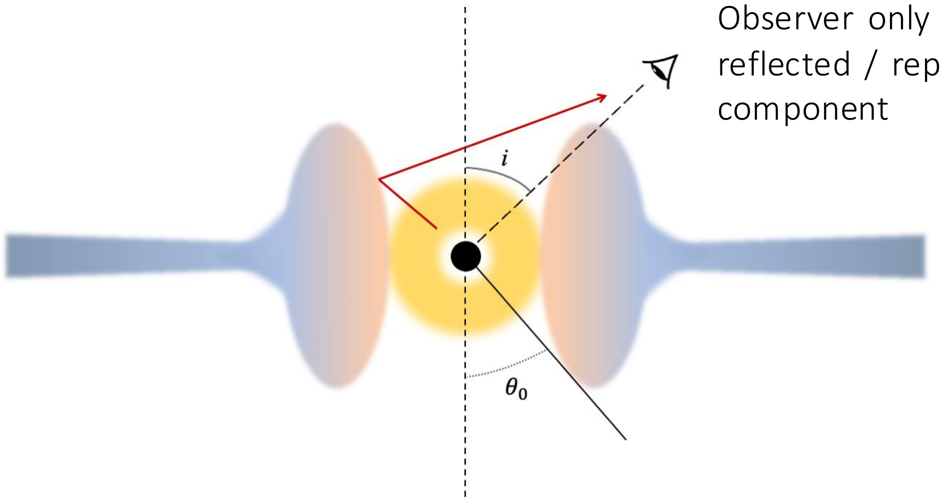

Observer only sees the reflected / reprocessed component

Gibaud et al. 2026

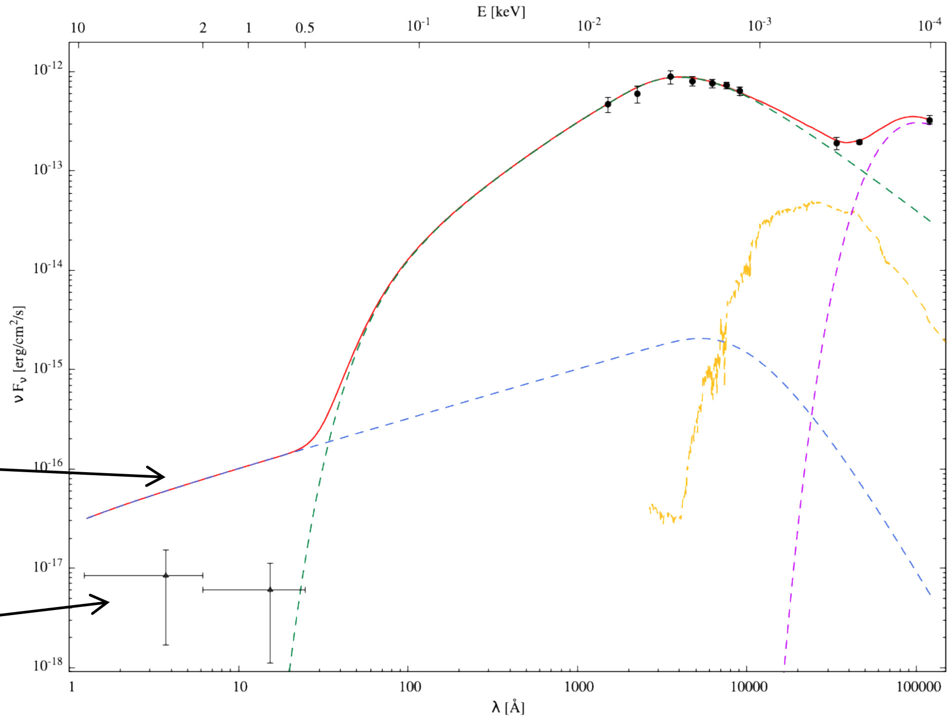

Intrinsic X-ray flux

X-ray flux we see

The accretion regime

X-ray binaries analogy

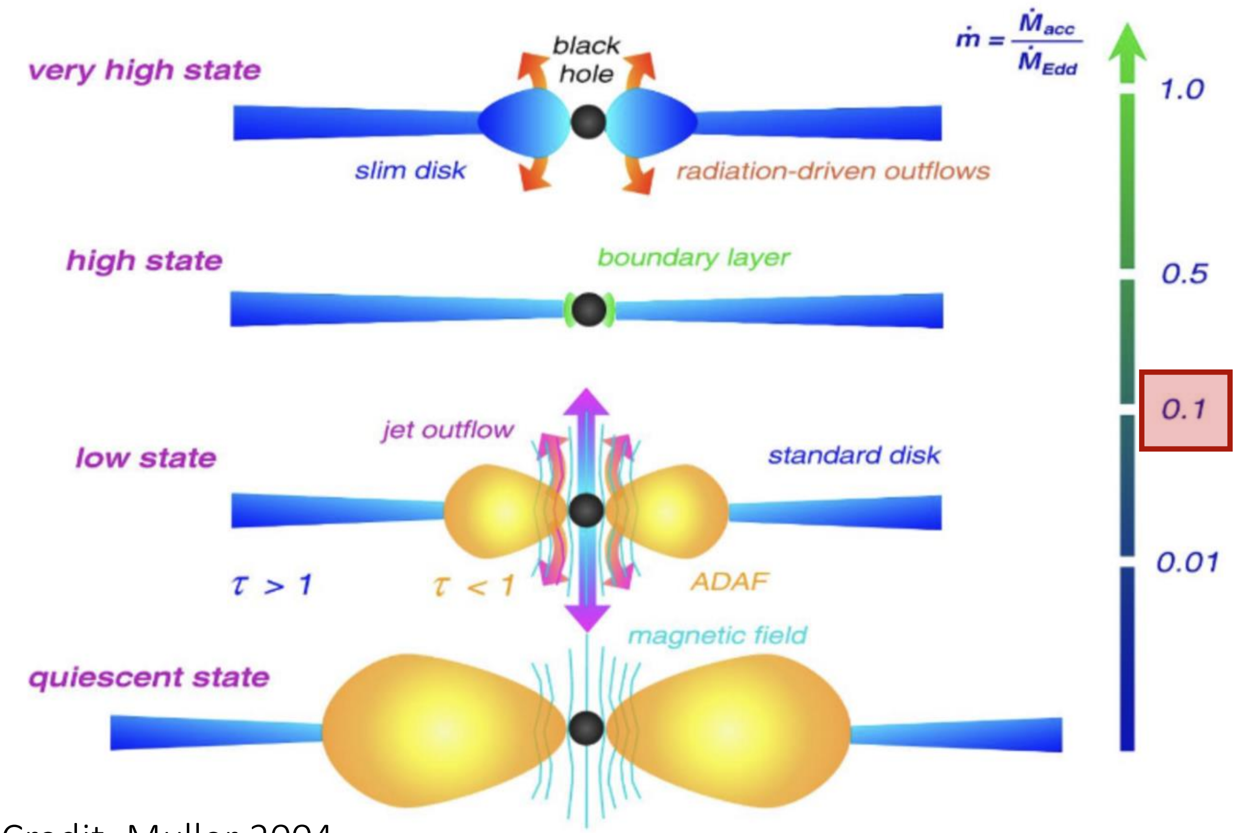

Credit: Muller 2004

High/soft state

- Standard accretion disk dominates => thermalized disk emission (soft X-rays, UV)
- Suppressed jets

Low/hard state

- Prominent hot corona => hard X-ray emission
- Hot inner flow
- Jets

Luminosity ratios for **model 1**

C IV / Mg II
C III] / Mg II

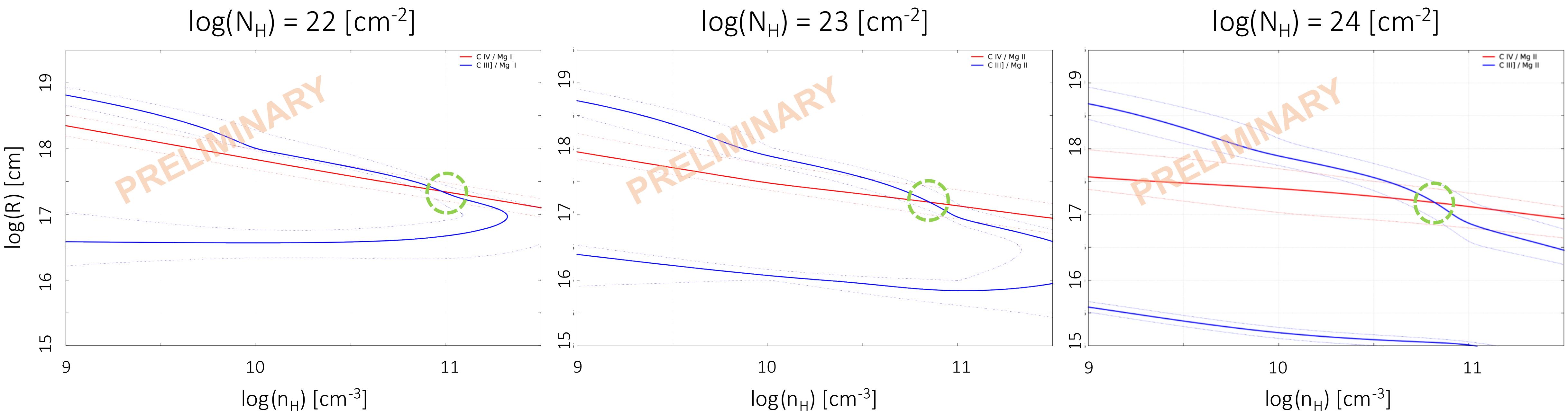

The 2 luminosity ratios agree with a narrow parameter range:

- $\log(n_H) \approx$ **10.9** $[cm^{-3}]$
- $\log(R) \approx$ **17.2** [cm]

Luminosity ratios for **model 2**

C IV / Mg II
C III] / Mg II

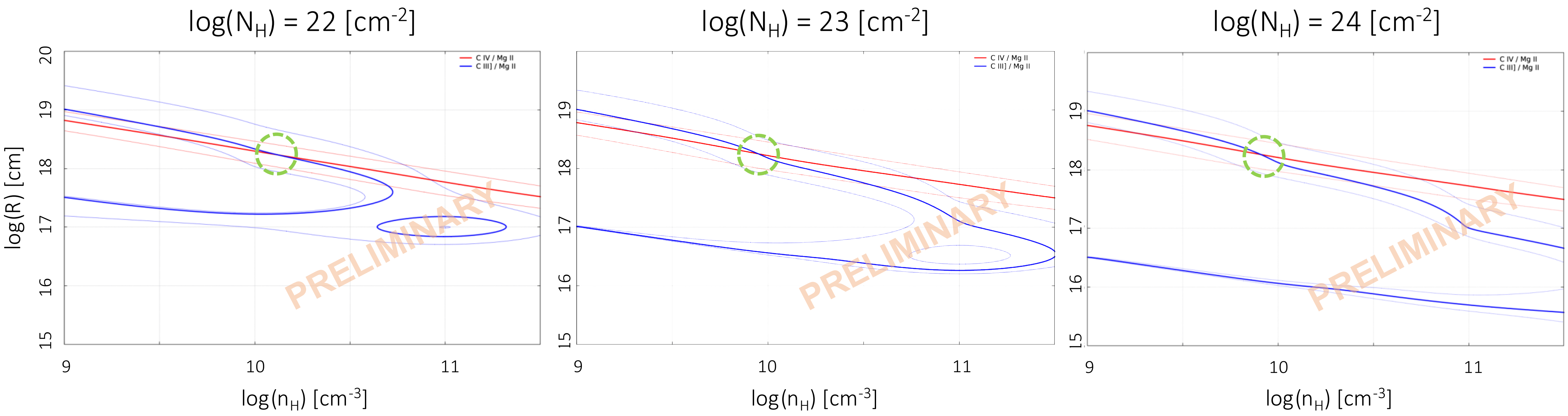

The 2 luminosity ratios agree with a narrow parameter range:

- $\log(n_H) \approx$ **10.0** $[cm^{-3}]$
- $\log(R) \approx$ **18.2** [cm]

EW of MgII emission line for **model 1**

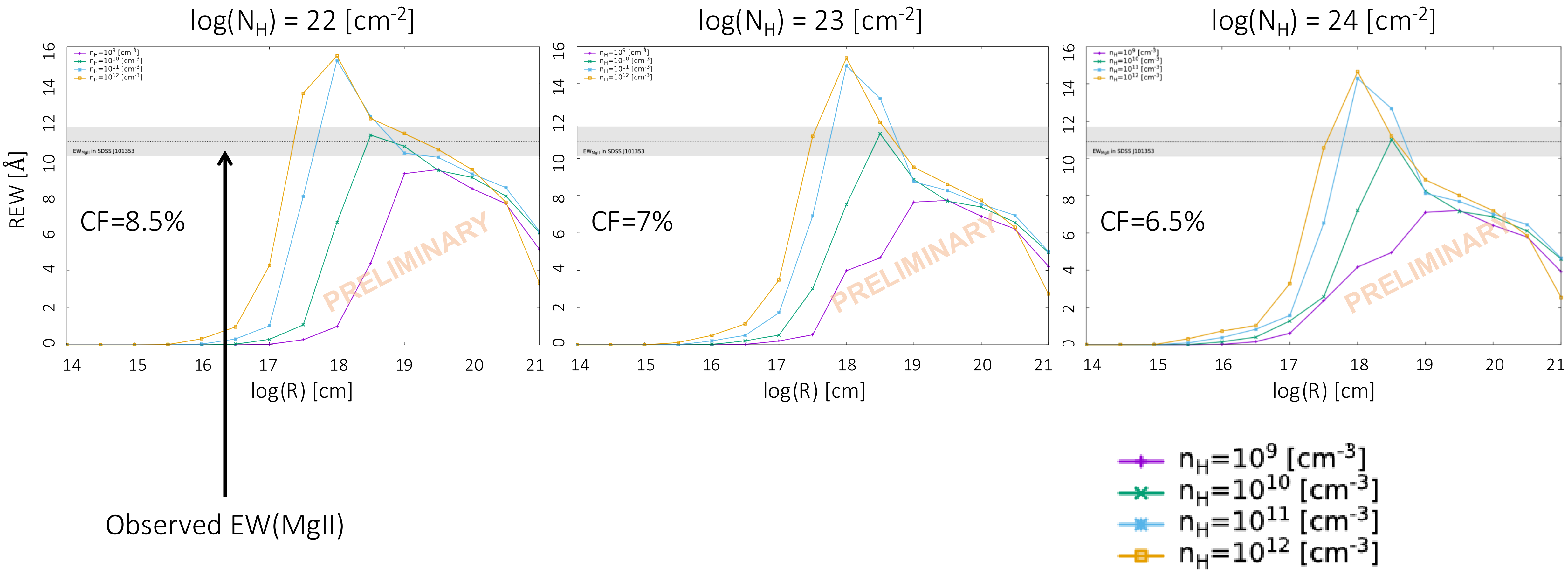

EW of MgII emission line for **model 2**